LA-UR-19-22920
Approved for public release; distribution is unlimited.

Title: Synthesis and luminescence of the BaFCl:Eu2+ scintillator system

Author(s): Richards, Cameron Gregory

Intended for: Report

Issued: 2019-04-01

Synthesis and luminescence of the BaFCl:Eu^{2+} scintillator system

CAMERON G. RICHARDS,[1,2,*]

[1]*Graduate Research Intern, MST-7 Engineered Materials, Los Alamos National Laboratory, Bikini Atoll Rd., SM 30, Los Alamos, NM 87545, USA*
[2]*Optical Materials and Devices, Masters Industrial Internship Program, 1252 University of Oregon Eugene, OR 97403, USA*
**crichar7@uoregon.edu*

Abstract: X-ray imaging capabilities play a vital role in the medical industry, thus incentivizing the need for advanced device development. BaFCl:Eu^{2+} is a promising material for scintillating composites applicable to pixelated X-ray imaging technology. Crystalline Eu(II)-doped BaFCl was synthesized via flux growth techniques with commercial reagents. The synthesis yield was separated into particle size subsets, and photo-luminescence (PL) spectra were obtained for each particle size range. Under UV irradiation, electronic transitions centered at 365 nm, 390 nm, and 430 nm were observed. Particle sizes <38 µm showed a significant drop in the characteristic Eu^{2+} ion emission and a more intense emission near 430 nm. X-ray diffraction (XRD) analysis revealed the presence of a secondary phase, $Ba_{12}F_{19}Cl_5$, and demonstrated that the introduction of this phase is dependent on synthesis parameters.

1. Introduction

1.1 Ionizing Radiation Detection in the Medical Industry

Following the discovery of the X-ray by Wilhelm Röntgen in 1895, the use of ionizing radiation (X-ray, γ-ray) as a tool for probing the inner structures of organic and inorganic materials is well known [1,4]. X-ray computed tomography (CT) scanners are critical diagnostic tools in the medical industry that have been shown to be extremely effective for studying the internal structures of patients.

Historically, there are two popular detection methods for radiography. These methods capitalize on the luminescent properties of phosphor materials to convert visible light to electronic signals which can be analyzed with computer algorithms. The first method involves the use of a phosphor plate that absorbs incident ionizing radiation and subsequently emits visible photons onto a pixelated camera system. The second method utilizes a storage phosphor that absorbs incident ionizing radiation and creates meta-stable states; these states are spatially released via optical stimulation, producing visible light through electron-hole recombination, and picked up by a PMT or Si-based photodetector. Since the image produced by the readout electronics is heavily dependent on the light generation ability of the phosphor material, improving this parameter is key to producing higher quality images.

Due to the severe health risks associated with prolonged exposure to ionizing radiation, minimizing the patient dose is a vital component in design considerations. Current technology can either suffer from optical data storage loss and/or poor spatial resolution; consequently, these drawbacks may lead to prolonged exposure [1].

In this paper, we explore a pixelated scintillating composite concept for the application of radiography; furthermore, we focus on the development of Eu(II)-doped BaFCl as the luminescent center for the composite technology.

1.2 Scintillator Technology

Scintillator materials are evaluated through their response characteristics; these characteristics are defined as the light yield, decay time, peak emission wavelength, and effective atomic number. The effective atomic number inherently dictates the materials ability to absorb high energy radiation; this property is related to the stopping power. Many modern scintillators, applicable to X-ray detection, contain heavy host constituents and are doped with luminescent ions. Heavy host constituents contribute largely to the X-ray interaction rate. Peak emission wavelength refers to the wavelength value where the maximum amount of light is emitted by the scintillator. The emission process is generally caused by the recombination of electron-hole pairs created by incident ionizing radiation. The decay time is representative of the time it takes for a scintillation event to reduce by a factor of $1/e$. If a scintillator has a long decay time (on the order of milliseconds), this can affect subsequent measurements made by the photodetector and can increase the overall image acquisition time. Current theory for predicting light yield suggests that it is dependent on the energy deposited from ionizing radiation, the band gap energy of the scintillator, the quantum efficiency, and the migration of electron-hole pairs to recombination centers [2].

In summary, ideal X-ray scintillators possess a large effective atomic number, high light yield, fast decay time (micro- to nanosecond), and peak emission wavelengths in the visible spectrum to match with current PMT's or Si-based photodetectors [3].

1.3 BaFCl:Eu^{2+} Properties

While there are many scintillators which possess ideal properties, we focus on Eu(II)-doped BaFCl for its technical maturity. First reported as a potential candidate for use with X-ray intensifying screens in 1975, the alkali-earth fluoro-halides (BaFCl:Eu^{2+}, BaFBr:Eu^{2+}) showed great potential due to a relatively high light yield in the blue end of the visible spectrum and a sufficiently high quantum efficiency [4]. Under UV excitation, BaFCl:Eu^{2+} emissions have been observed at 365 nm, 385 nm, and 430 nm on numerous occasions [4-6, 8-11]. These emission wavelengths make BaFCl:Eu^{2+} well suited photodetector readout. The emissions at 365 nm and 385 nm are attributed to the $^6P_{7/2} \rightarrow {}^8S_{7/2}$ and $4f^6 5d^1 \rightarrow {}^8S_{7/2}$ transitions of the Eu^{2+} ion, respectively. The emission at 430 nm has been reported to be due to impurity contributions or the presence of a secondary phase of the barium halide system [5, 10, 14]. Existing literature also reports that the decay times of these transitions are in the µs regime [6]. Collectively, these properties suggest good detection material candidacy.

1.4 Scintillating Composite Approach

In order to fabricate the proposed BaFCl:Eu^{2+} scintillating composite, micron sized BaFCl:Eu^{2+} particles will be mixed with an index-matching polymer binder; here, this study looks at UV curable adhesives. Through matching the refractive indices, one can improve scintillation light transport through a composite material and reduce the number of scattering events. *Cusano et al* investigated a similar composite concept through high pressure fabrication routes [8]. In figure [1], the index of refraction of BaFCl:Eu^{2+} is plotted as a function of wavelength. From the figure, we can see that for emissions between 380 nm-450 nm, the index lies between 1.66 and 1.69, which is well matched to commercially available optical adhesives such as those available by Norland Products. These adhesives can potentially be mixed to control the optical properties of the composite.

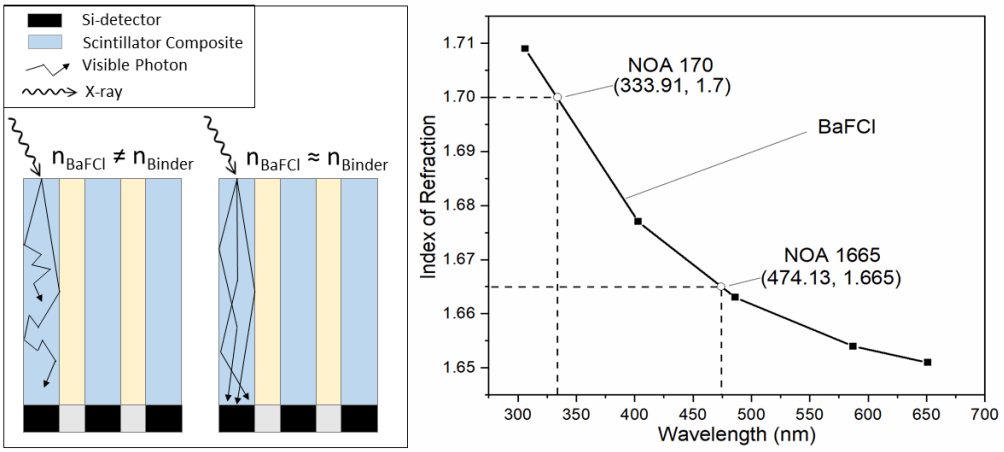

Fig. 1. Left: Schematic drawing of the composite scintillator approach. As depicted, photons in a non-index matched composite will encounter significantly more scattering events than in an index matched composite, leading to a degradation of image quality in the non-index matched composite. Right: Index of refraction for BaFCl:Eu^{2+} as a function of wavelength. Indices for various Norland Optical Adhesives are labeled.

2. Experimental

The synthesis of BaFCl:Eu^{2+} was performed by mixing BaF_2(s), $BaCl_2$(s), and EuF_2(s) and melting them under inert atmosphere to form the BaFCl:Eu^{2+} compound upon cooling. The melting points of BaF_2 and EuF_2 (1368 ˚C and 1380 ˚C, respectively) are much higher than that of $BaCl_2$ (962 ˚C). The synthesis therefore uses a 20 mol% excess of $BaCl_2$ which, when molten at a process temperature of 1100 ˚C in a carbon crucible, acts as a flux to dissolve BaF_2 and EuF_2. Complete dissolution of BaF_2 and EuF_2 is essential before cooling the melt, and it is determined by the soaking time. Soaking times of 4 hours (trial 1) and 12 hours (trial 2) at 1100 ˚C were explored.

The resulting yields were subsequently crushed and filtered with DI water to remove excess $BaCl_2$. Following the washing process, the remaining material was collected and annealed at 120 ˚C for 18 hours, in ambient atmosphere, to remove residual moisture. Energetic ball milling was also explored to investigate the effects on luminescence with respect to ball milling.

The BaFCl:Eu^{2+} crystalline powder was then size-separated using a multi-layered sieve with mesh layers of 75 µm, 53 µm, and 38 µm. Representative photoluminescence (PL) spectra were taken for each synthesis trial using a Photon Technology Inc. fluorescence spectrometer. PL spectra were also obtained over a range of excitations for each particle size subset. Each synthesis trial was investigated through X-ray diffraction techniques to determine the material phase composition.

3. Results and Discussion

3.1 Photoluminescence of BaFCl:Eu^{2+} Powder Samples

Comparing the PL emissions of trial 1 and trial 2 showed significant differences, as seen in figure [2]. Irradiation with 334 nm light produced emission peaks at 362 nm and 383 nm for trial 1, and displayed emission peaks at 362 nm and 394 nm with a shoulder near 430 nm for trial 2. The distinct change in the emission spectra clearly indicates the soaking time is a significant variable affecting the product.

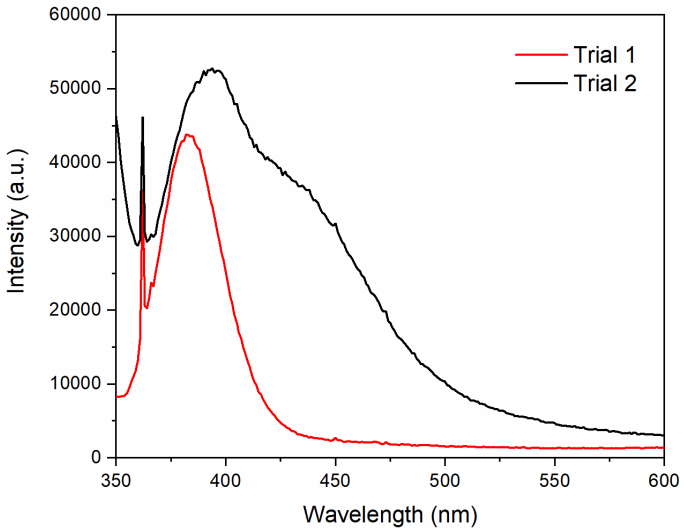

Fig. 2. Photoluminescence of representative BaFCl:Eu^{2+} powder from each synthesis trial under 334 nm irradiation.

3.2 Ball Milling Study with Trial 1

BaFCl:Eu^{2+} powder obtained from trial 1 was milled with 200 mL of Liquinox® solution for 24 hours. The admixture was then transferred to glass containers and centrifuged at 1000 rpm for 10 min. Following the centrifuge process, each container was annealed at 95 ˚C for 16 hours and subsequently at 120 ˚C for 8 hours. The dehydrated powder was sieved for 4 hours. Figure [3] displays the effects of ball milling on the PL properties. As shown in the figure, milling with the Liquinox® solution, followed by drying, reduced the emission intensity by approximately 30 percent compared to the as-synthesized powder. The reduction in emission intensity was nearly equal for both small and large milled particles, indicating an overall quenching of the luminescent properties of Eu^{2+} in the BaFCl system.

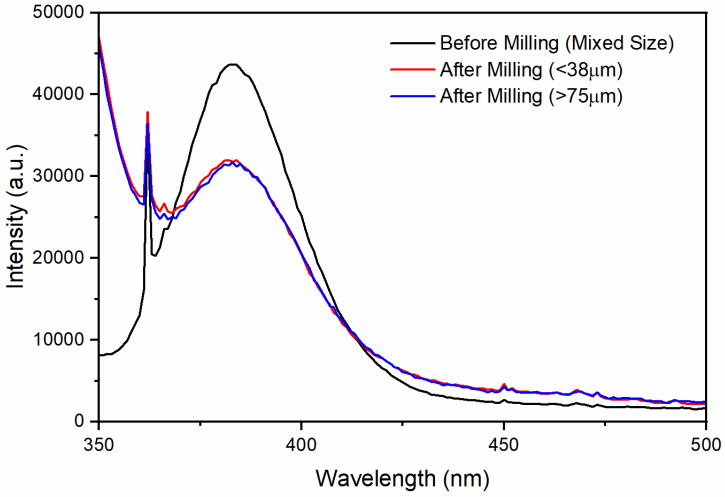

Fig. 3. Photoluminescence of BaFCl:Eu^{2+} powder under 334 nm irradiation before and after milling, The figure displays a reduction of light output after the milling process.

3.2 Particle Size Study with Trial 2

Based on the different emission characteristics from trial 1, the BaFCl:Eu^{2+} powder from trial 2 was also sieved and investigated by PL. The emission spectra for each particle size subset is shown in figure [4] (left). From the figure, it is clear that there is a significant relationship between particle size and the PL properties; each spectra includes a feature at 430 nm, which increases in intensity with decreasing particle size. Adjacent to the emission spectra shown in figure [4] is a plot showing the linear trend of each peak emission wavelength as a function of particle size.

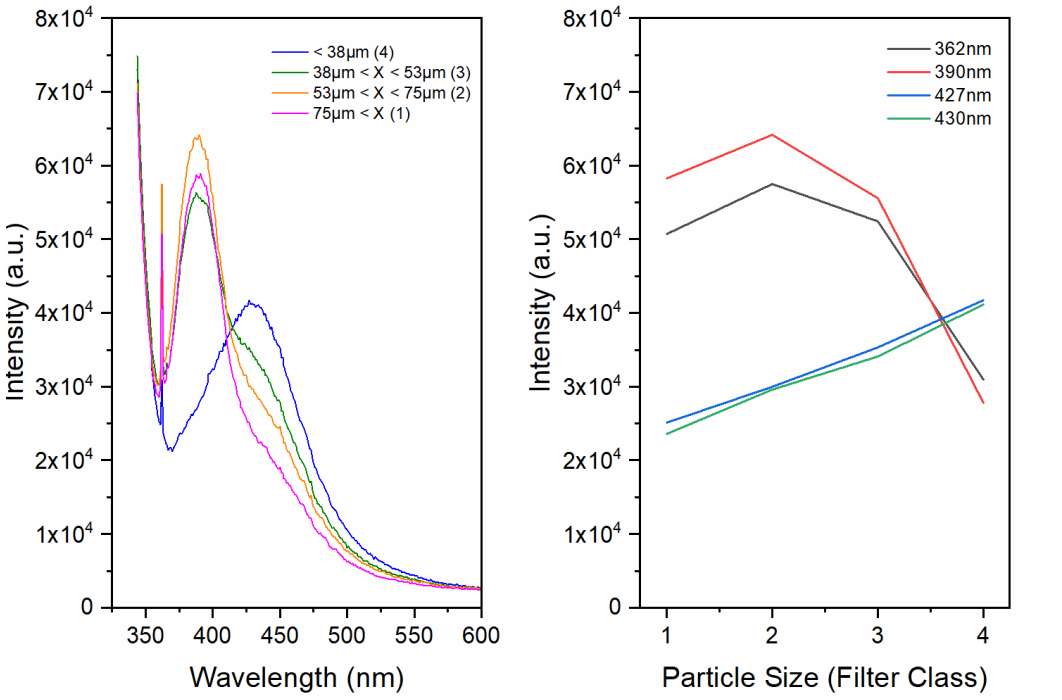

Fig. 4. Photoluminescence of BaFCl:Eu2+ powder from trial 2, under 334 nm irradiation, separated by particle size subsets. Left: PL emissions as a function of wavelength. Right: PL emissions as a function of particle size subsets; note that filter class 1 contains the largest particles and filter class 4 contains the smallest particles.

Due to the varying PL characteristics, observed from the particle size subsets, further PL studies were conducted to explore the transition at 430 nm. Particle size subsets 1 and 4 were analyzed with an excitation range, as shown in figure [5]. In the contour images, it can be seen that subset 1, in triangle (a), displays an interplay between two emission bands for a wide range of excitations; as the excitation energy decreases, emissions in the range of 400 to 450 nm increases. The data in subset 4, in triangle (b), displays a relatively static emission over the excitation range 300 to 350 nm.

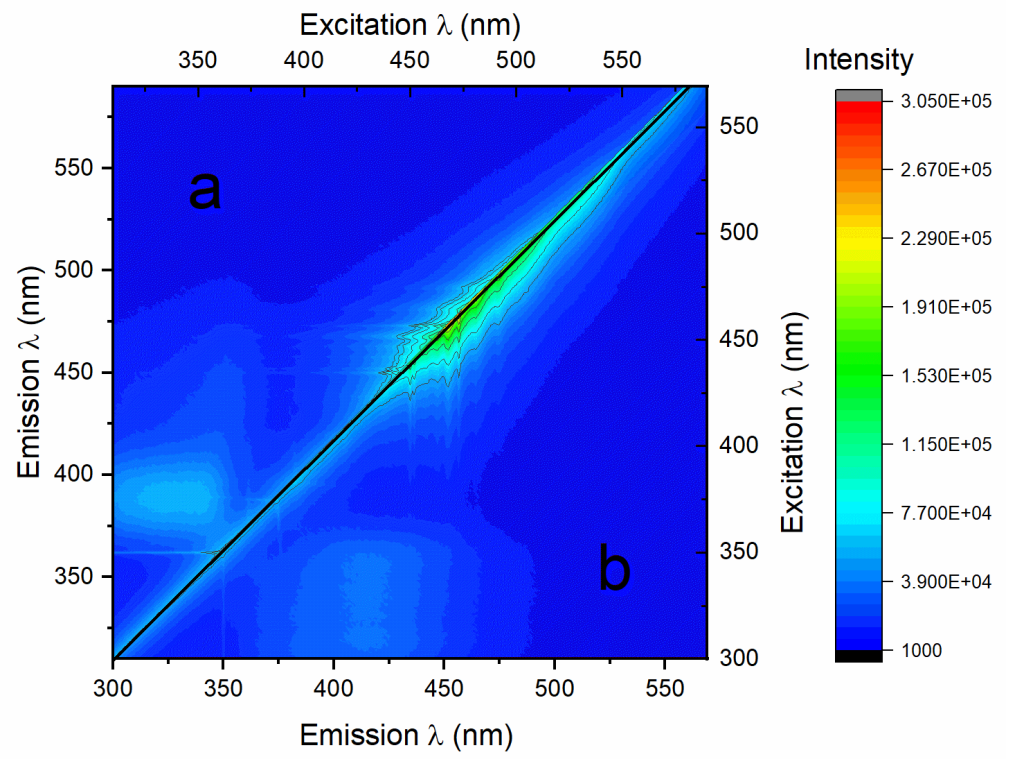

Fig. 5. 2D emission contour for the BaFCl:Eu^{2+} powder from trial 2. The contour plot in triangle (a) displays the PL features for the largest sized particles (>75 μm), and the contour plot in triangle (b) displays the PL features for the smallest size particles (<38 μm). The black line on the diagonal separates the two contours. The notable features can be seen in the bottom left hand corner; specifically, contour (a) demonstrates an excitation dependent emission range while contour (b) shows a constant emission range centered at 430 nm.

The peak emissions at 362 nm and 390 nm can be related to the electronic transitions of the Eu^{2+} ion, namely the $^6P_{7/2} \rightarrow {}^8S_{7/2}$, $4f^6 5d^1 \rightarrow {}^8S_{7/2}$ transitions, respectively. Previous studies on the PL emissions of BaFCl:Eu^{2+} attribute the 430 nm emission to oxygen impurity sites within the lattice [5, 10]; however, the presence of a secondary phase can also shift emissions through crystal field effects [12]. To elucidate the origin of the 430 nm emission, X-ray diffraction techniques were employed.

3.3 X-Ray Diffraction

Each synthesis trial of BaFCl:Eu^{2+} powder was irradiated with Cu-Kα (0.154059 nm) X-rays. The measured spectra were compared with a calculated powder pattern based on material phase information [13]. The result of the XRD analysis, shown in figure [6], confirmed the presence of a secondary phase of the barium halide system in trial 2. The secondary phase, $Ba_{12}F_{19}Cl_5$, was calculated to be the majority phase for particle size subset 4. Supporting this evidence, a study on the photoluminescence of Eu^{2+} ions in various host lattices has shown that an emission at 434 nm in a BaFCl:Eu^{2+} system is a result of the $Ba_{12}F_{19}Cl_5$ phase [14]. Thus, we can attribute the 430 nm PL emission observed in trial 2 to a secondary phase contribution. One explanation for the secondary phase being present in trial 2 can be due to the longer soaking time. Due to the fact that $BaCl_2$ has a large vapor pressure at 1100 ˚C, the volatile loss of $BaCl_2$ can create a BaF_2 rich environment leading to the formation of the $Ba_{12}F_{19}Cl_5$ phase during cool down.

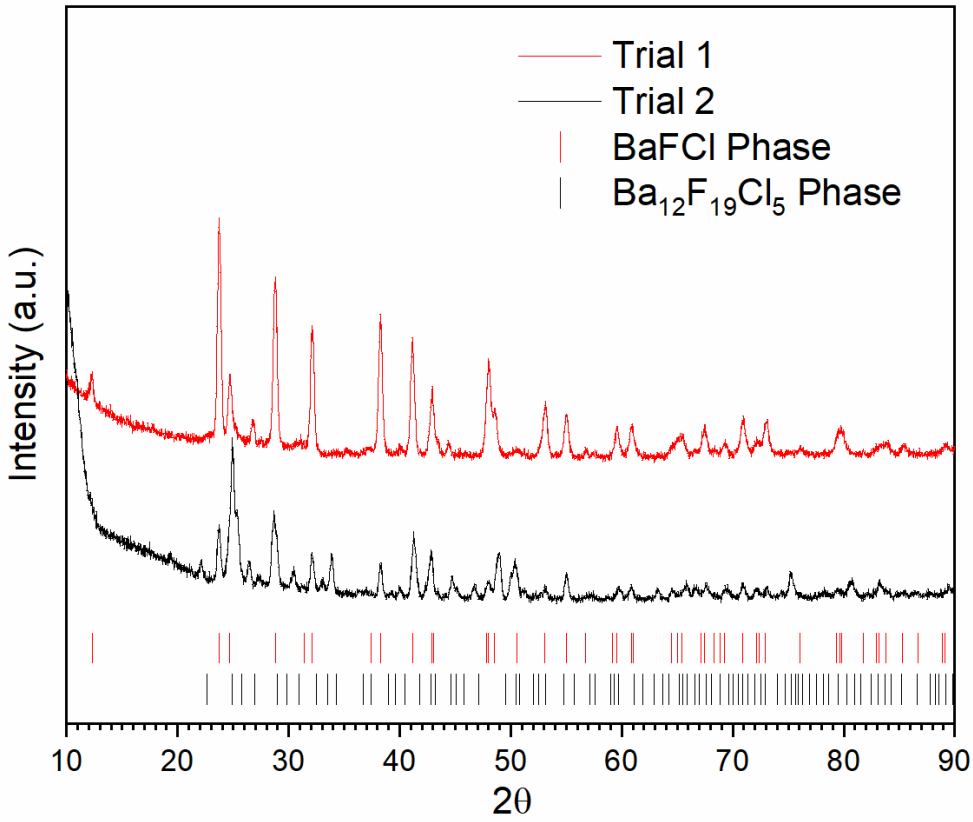

Fig. 6. XRD spectra of particle sizes <38 µm. $Ba_{12}F_{19}Cl_5$ is present in Trial 2 due to the differences in the primary diffraction peaks. Signature diffraction peaks for BaFCl and $Ba_{12}F_{19}Cl_5$ are included below the traces in vertical lines.

4. Conclusion

We have investigated the synthesis of Eu(II)-doped BaFCl through flux growth techniques with BaF_2(s), $BaCl_2$(s), and EuF_2(s) reagents. This method could be scaled up to produce vast amounts of scintillating powder. The resulting crystalline powder contains various sized particles, each having unique emission characteristics. It was also shown that ball milling with Liquinox® solution induces quenching of the Eu^{2+} ion luminescence. Under UV irradiation, peak emissions at 362 nm, 390 nm, and 430 nm were observed; these peak emission can be accredited to the $^6P_{7/2} \rightarrow {}^8S_{7/2}$, $4f^65d^1 \rightarrow {}^8S_{7/2}$ electronic transitions of the Eu^{2+} ion and a transition related to the $Ba_{12}F_{19}Cl_5$ phase, respectively. XRD analysis determined that the generation of the $Ba_{12}F_{19}Cl_5$ phase can be controlled through soaking time during the synthesis.

Funding

Funding for this project was provided by Los Alamos National Laboratory.

Acknowledgments

Special thanks to Dr. Brenden Wiggins for mentorship and introduction into the scintillator field.

References

1. M. Körner, C. H.Weber, S. Wirth, K. Pfeifer, M. F. Reiser, and M. Treitl, "Advances in Digital Radiography: Physical Principles and System Overview," RadioGraphics **27**(3), 675-686 (2007).
2. Yanagida, Takayuki. "Inorganic scintillating materials and scintillation detectors" *Proceedings of the Japan Academy. Series B, Physical and biological sciences* **94**(2), 75-97 (2018).

3. P. Leblans, D. Vandenbroucke, and P. Willems, “Storage Phosphors for Medical Imaging,” *Materials (Basel, Switzerland)* **4**(6), 1034-1086 (2011).
4. A. L. N. Stevels and F. Pingault, “BaFCI :Eu2+, A NEW PHOSPHOR FOR X-RAY INTENSIFYING SCREENS,” *Philips Research Reports* **30**(5), 277-290 (1975).
5. W. Chen, N. Kristianpoller, A. Shmilevich, D. Weiss, R. Chen, and M. Su, “X-Ray Storage Luminescence of BaFCl:Eu^{2+} Single Crystals,” *The Journal of Physical Chemistry* **B 109**(23), 11505-11511 (2005).
6. M. Secu, C. E. Secu, V. Vasile, D. Predoi, and D. M. Gazdaru, “Time-resolved luminescence spectroscopy of Eu2+ in BaFCl:Eu2+ X-ray storage phosphor,” *Journal of Optoelectronics and Advanced Materials* **9**(6), 1800-1802 (2007).
7. F. Kubel, H. Hagemann, and H. Bill, “Synthesis and Structure of $Ba_{12}F_{19}Cl_5$,” *Zeitschrift fur anorganische und allgemeine Chemie,* **622**(2), 343-347 (1996).
8. D. A. Cusano, R. K. Swank, P. J. White, “INDEX-MATCHED PHOSPHOR SCINTILLATOR STRUCTURES,” *United States Patent Office,* Patent US4316817A (1982).
9. X. Meng and J. Zhou, “Photostimulated luminescence of BaFCl:Eu^{2+} in oxide glass ceramics,” *Proc. SPIE 7658,* 765847 (2010).
10. M. Secu, L. Matei, T. Serban, E. Apostol, Gh. Aldica, and C. Silion, “Preparation and optical properties of BaFCl:Eu^{2+} X-ray storage phosphor,” *Optical Materials* **15**, 115-122 (2000).
11. W. Chen, Z. Wang, L. Lin, and M. Su, “NEW COLOR CENTERS AND PHOTOSTIMULATED LUMINESCENCE OF BaFCl:Eu^{2+},” *Journal of Physics and Chemistry of Solids* **59**(1), 49-53 (1998).
12. M. Fox, “Optical Properties of Solids,” *Oxford University Press, 186-202 (2001).*
13. M. Sauvage, “Refinement of the Structures of SrFCl and BaFCl,” *Acta Crystallographica,* **30**(11), 2786-2787 (1974).
14. B. Es-Sakhi, A. Garcia, L. Struye, P. Willems, P. Leblans, A. Moudden, and C. Fouassier, “Photoluminescence of Eu^{2+} in BaF_2-rich Fluorohalides and photostimulation after X-ray irradiation,” *Materials Science and Engineering,* **B**(96), 233-239 (2002).